

Supplementary Information for:

**Expanding the DNA Damaging Potential of Artificial
Metallo-Nucleases through Click Chemistry**

Alex Gibney,^a Margareth Sidarta,^{b,c} Sriram KK,^b Obed Akwasi Aning,^{b,c} Lily Arrué,^d Francisca Figueiredo,^e Pierre Mesdom,^e Kevin Cariou,^e Pegah Johansson,^{f,g} Shayon Bhattacharya,^d Damien Thompson,^d Vickie McKee,^{a,h} Michaela Wenzel,^{b,c} Gilles Gasser,^e Fredrik Westerlund,^{b,c} and Andrew Kellett^{a*}

[a] Research Ireland Centre for Pharmaceuticals, School of Chemical Sciences, Dublin City University, Glasnevin, Dublin 9, Ireland.

Andrew.kellett@dcu.ie

[b] Department of Life Sciences, Chalmers University of Technology, Gothenburg, Sweden.

[c] Centre for Antibiotic Resistance Research in Gothenburg (CARE), Gothenburg, Sweden

[d] Research Ireland Centre for Pharmaceuticals, Department of Physics, University of Limerick, Ireland.

[e] Chimie ParisTech, PSL Université, CNRS, Institute of Chemistry for Life and Health Sciences, Paris, France.

[f] Department of Clinical Chemistry, Sahlgrenska University Hospital, Region Vastra Gotaland, Gothenburg, Sweden.

[g] Department of Laboratory Medicine, Institute of Biomedicine, Sahlgrenska Academy at University of Gothenburg, Sweden.

[h] Department of Physics, Chemistry and Pharmacy, University of Southern Denmark, Campusvej 55, 5230 Odense M, Denmark.

28	Table of Contents	
29	General Remarks	3
30	Synthesis	3
31	Crystallography	5
32	Verification of In-Situ Complexation by ESI-MS	5
33	Fluorescence Quenching	5
34	Microscale Thermophoresis	5
35	Fluorescence Melting	6
36	Single Molecule Analysis – DNA Binding	6
37	Docking Studies	6
38	Molecular Dynamics	6
39	Characterisation of interactions	7
40	National Cancer Institute 60 Cell Line Screening (NCI-60)	7
41	ICP-MS Studies of Intracellular Cu	7
42	Bacterial Assays	8
43	<i>Bacterial growth conditions and compounds preparation</i>	8
44	<i>Bacterial cytological profiling (BCP)</i>	8
45	<i>BCP image analysis</i>	8
46	<i>Bacterial chromosomal DNA preparation</i>	8
47	Pulse field gel electrophoresis (PFGE)	8
48	Bacterial DNA fluorescence microscopy	9
49	DNA Cleavage by Agarose Gel Electrophoresis	9
50	Repair Assisted Damage Detection	10
51	Blood Sample Collection	10
52	Treatment of PBMCs with Cu(II)-TC-Py and antioxidants	10
53	Extraction of DNA	10
54	Fluorescent labeling of CU(II)-TC-Py induced DNA damage	10
55	Silanization of coverslips	10
56	Stretching of DNA and imaging	10
57	Software analysis	11
58	Statistics	11
59	Supplementary Figures and data:	12
60	References:	32
61		
62		

63 General Remarks

64 Chemicals and reagents were sourced from Sigma-Aldrich and Tokyo Chemical Industry (TCI) and were
65 used without any further purification. HPLC grade chloroform and methanol were used without further
66 purification. ¹H and ¹³C NMR spectra were obtained on a Bruker AC 600 MHz NMR spectrometer and
67 processed in MNova (MastreLab). Thermal melting analysis was performed on a Roche LightCycler 480
68 II. Fluorescence quenching assays were performed using commercial EtBr, Hoechst 34580 (sigma) and
69 Methyl green (TCI) and plates were read on a TECAN Spark® microplate reader. Circular dichroism data
70 was collected on an Applied Photophysics Chirascan Plus. Microscale thermophoresis experiments were
71 conducted on a Nanotemper Monolith® instrument using standard capillaries. Human topoisomerase I
72 was acquired from Sigma.

73

74 **Caution!** Sodium azide is acutely toxic and is an explosion hazard. Refer to organic azide stability prior
75 to the preparation of any azide compounds. The total number of nitrogen atoms in a final organic azide
76 should not exceed that of carbon. Organic azides with a C/N ratio of <1 should never be isolated. It may
77 be synthesised if the azide is a transient intermediate species and the limiting reagent in the reaction
78 mixture has a maximum quantity of 1 g. Each azide compound should be individually evaluated.

79

80 Synthesis

81 TC Ligands were prepared using the copper catalysed alkyne-azide cycloaddition (CuAAC) of 2,4,6-
82 Tris-(azidomethyl)-mesitylene (Triazide) with a variety of commercially available alkynes in the presence
83 of the co-catalyst tris-hydroxypropyltriazolylmethylamine (THPTA). In all cases the aqueous solutions of
84 active catalyst was prepared in situ by dissolving appropriate quantities of Cu(II) sulphate (1 mol %) and
85 THPTA (1 mol %) in 0.5 mL of water followed by addition of 0.5 mL aqueous Na-L-ascorbate (5 mol %).

86

87 2,4,6-Tris-(azidomethyl)-mesitylene (triazide):

88 Synthesis was modified from previously reported procedure To a solution of 2,4,6-tris-(bromomethyl)-
89 mesitylene (1.025 g, 2.56 mmol) in acetone (50 mL) sodium azide (1.00 g, 15.38 mmol) was added in
90 portions over ice over a period of 20 min. (Caution! Sodium azide is acutely toxic and is an explosion
91 hazard. Refer to organic azide stability prior to the preparation of any azido compounds). The reaction
92 was refluxed overnight and allowed to cool to room temperature. The suspension was gravity filtered and
93 the filtrate was dried under reduced pressure to yield the title product as a crystalline white solid. NMR
94 data was in line with previously reported results.

95 (((2,4,6-trimethylbenzene-1,3,5-triyl)tris(methylene))tris(1H-1,2,3-triazole-1,4-diyl))trimethanol 96 (TC-OH):

97 The active catalyst solution was added to a solution of triazide (100mg, 0.35mmol) in DMF (5 mL) and
98 allowed to stir for 10 minutes. The resulting solution was then added dropwise to a stirring solution of
99 propargyl alcohol (196mg, 3.5mmol) in DMF (5mL). The flask was flushed with nitrogen and allowed to
100 stir overnight at room temperature. The bright yellow solution was dried under a stream of nitrogen. The
101 yellow solid was suspended in acetone (5mL) with sonication. The title product (125mg, 81%) was iso-
102 lated by vacuum filtration and washing with ice cold acetone (5 x 5 mL). ¹H NMR (DMSO, 600 MHz): δ
103 2.42 (s, 9H) 4.48 (d, 6H, J = 5.5 Hz) 5.13 (t, 3H, J = 5.5 Hz) 5.66 (s, 6H) 7.76 (s, 3H). ¹³C NMR (DMSO,
104 151 MHz) δ: 16.78, 48.73, 55.45, 122.80, 131.42, 139.64, 148.36. ESI-MS positive ionization mode:

105 [M+H]⁺ Calculated m/z = 454.23 found m/z = 454.23, [M+Na]⁺ calculated m/z = 476.21 found m/z =
106 476.21.

107 **1,1',1''-((2,4,6-trimethylbenzene-1,3,5-triyl)tris(methylene))tris(1H-1,2,3-triazole-4-carboxylic acid)**
108 **(TC-Acid):**

109 The active catalyst solution was added a solution of triazide (100mg, 0.35mmol) in methanol (10 mL) and
110 stirred at room temperature for 10 minutes. The resulting solution was added dropwise to a solution of
111 propionic acid (98 mg, 1.4mmol) in methanol (5 mL). The reaction flask was flushed with nitrogen, sealed
112 and the reaction was stirred vigorously overnight. A white precipitate was removed by vacuum filtration.
113 The filtrate was dried under reduced pressure to yield a white solid that was then suspended in acetone
114 (5mL) with sonitcation and isolated by decanting. The remaining solid was dried over desicant to yield
115 the title product as a white solid. Yield = 145mg (83 %). ¹H NMR (DMSO 600 MHz): δ 2.38 (s, 9H), 7.74
116 (s, 6H) 8.55 (s, 3H) 13.14 (s, 3H) ESI-MS (negative ionization mode): ESI-MS negative ionization mode:
117 [M + H]⁺ calualted m/z = 496.17 found m/z = 496.17. [M+Na]⁺ calculated m/z = 518.15 found m/z =
118 518.15.

119 **1,1',1''-((2,4,6-trimethylbenzene-1,3,5-triyl)tris(methylene))tris(1H-1,2,3-triazole-4-carboxamide)**
120 **(TC-Amide):**

121 The active catalyst solution was added a solution of triazide (159.2mg, 0.56mmol) in degassed ACN
122 (8mL). The mixture was allowed to stir for 15 minutes before the dropwise addition of propiolamide
123 (115mg, 1.67 mmol). The reaction mixture was allowed to stir at room temperature for 3 hours. The title
124 product was collected by vacuum filtration washed with cold acetonitrile (3 x 5 mL) and dried over desic-
125 cant. yield = 270mg (98 %). ¹H NMR (DMSO, 600 MHz): δ 2.38 (s, 9H), 5.74 (s, 6H), 8.34 (s, 3H). ESI-
126 MS: [M+Na]⁺ m/z calculated = 515.20 found m/z = 515.20.

127 **2,2',2''-(((2,4,6-trimethylbenzene-1,3,5-triyl)tris(methylene))tris(1H-1,2,3-triazole-1,4-diyl))tripyrim-**
128 **idine (TC-Pym):**

129 The active catalyst solution was added to a stirring solution of triazide (91mg, 0.32mmol) in methanol
130 (8mL). The mixture was allowed to stir at room temperature for 15 minutes before dropwise addition of
131 2-ethynyl pyrimidine (100mg, 0.96mmol) in methanol (1mL). The title product was isolated as a off-white
132 solid by vacuum filtration, washing with 5mL 0.1M aqueous EDTA solution and 5mL acetone. Yield =
133 170mg, 89%. ¹H NMR (DMSO, 600 MHz): δ 2.48 (s, 9H), 5.76 (s, 6H), 7.42 (t, 3H J = 4.96Hz) 8.57 (s,
134 3H), 8.83 (d, 6H, J = 4.88Hz). ESI-MS: [M+H]⁺ calculated m/z = 598.327 found m/z = 598.26 [M+Na]⁺
135 calculated m/z = 620.25 found m/z = 620.25

136 **2,2',2''-(((2,4,6-trimethylbenzene-1,3,5-triyl)tris(methylene))tris(1H-1,2,3-triazole-1,4-**
137 **diyl))tripyridine (TC-Py):** An activated catalyst solution consisting of 1mol% CuSO₄ and 5 mol% Na-L-
138 Ascorbate was added to a stirring solution of triazide (120mg, 0.42mmol) in methanol (8mL). The mixture
139 was allowed to stir at room temperature for 15 minutes before dropwise addition of 2-ethynyl pyridine
140 (132mg, 1.28mmol) in methanol (2mL). The reaction mixture was allowed to stir for 16 hours at room
141 temperature. The title product was isolated as a white solid by vacuum filtration and washing with 5mL
142 0.1M aqueous EDTA solution, 5mL acetone and 20 mL Et₂O. Yield = 225mg, 90%. ¹H NMR (DMSO, 600
143 MHz): δ 2.48 (s, 9H), 2.53 (s, 6H), 7.32 (m, 3H) 7.87 (td, 3H, J₁ = 7.4Hz, J₂ = 1.4Hz) 7.99 (dt, 3H, J₁ =
144 7.94 Hz, J₂ = 0.84 Hz) 8.38 (s, 3H) 8.54 (m, 3H). ESI-MS: Found [M+H]⁺ m/z = 595.28 calculated [M+H]⁺
145 = 595.28.

146 **2,2',2''-(((2,4,6-trimethylbenzene-1,3,5-triyl)tris(methylene))tris(1H-1,2,3-triazole-1,4-**
147 **diyl))tris(benzo[d]thiazole) (TC-Benzo):**

148 To a stirring solution of triazide (119mg, 0.4mmol) in methanol (20 mL) , were added solutions of CuSO₄
149 (5 mol%) and (+)-Sodium L-ascorbate (20 mol %) in water (0.5 ml each). The mixture was allowed to stir

for 15 minutes before being added dropwise to a solution of 2-ethynyl benzothiazole (200 mg, 1.2 mmol) in methanol (5 mL). The flask was flushed with nitrogen, sealed, and allowed to stir overnight at room temperature. A yellow precipitate formed. The reaction volume was reduced to 3 mL and the title product collected by vacuum filtration (310 mg, 99%). ¹H NMR (DMSO, 600 MHz): δ 5.85 (s, 6H), 7.45 (t, 3H, J = 7.41 Hz), 7.52 (t, 3H, J = 8.19 Hz), 7.97 (d, 3H, J = 7.73 Hz), 8.14 (d, J = 7.41 Hz), 8.79 (s, 3H) ESI-MS: [M+H]⁺ calculated = 763.20 found m/z = 763.19 [M+Na]⁺ calculated m/z = 785.18 found m/z = 785.18.

Crystallography

The data were collected at 100(1)K on a Synergy, Dualflex, AtlasS2 diffractometer using CuKα radiation (λ = 1.54184 Å) and the CrysAlis PRO suite.¹ Using shelXle² and Olex2³ the structure was solved by dual space methods (SHELXT⁴) and refined on F² using all the reflections (SHELXL-2019/2⁵). All the non-hydrogen atoms were refined using anisotropic atomic displacement parameters and hydrogen atoms were inserted at calculated positions using a riding model. Crystal parameters, data collection and structure refinement details are summarised in **Table S1**.

Verification of In-Situ Complexation by ESI-MS

Formation of TC-Cu₃ complexes *in-situ* was investigated using ESI-MS. Solutions of TC ligands were prepared in DMF prior to addition of three equivalents of aqueous Copper(II) nitrate trihydrate. Samples were vortexed and incubated at 37 °C for 30 minutes before further dilution (as required) and analysis on a MaXis HD quadrupole electrospray time-of-flight (ESIQTOF) mass spectrometer (Bruker Daltonik GmbH, Bremen, Germany), using a glass syringe (Hamilton) and syringe pump (KD Scientific, Model 781100) for infusions at a flow rate of 3 mL/min.

Fluorescence Quenching

Competitive ethidium bromide displacement was conducted as previously reported with slight modification.⁶ Briefly, a triplicate serial dilution of test compound was prepared on a 96 well plate to a volume of 50 µL. 50 µL of a working solution of EtBr (25.2 µM) and ctDNA (25 µM) was then added to give a final volume of 100 µL, 12.5 µM EtBr, 12.5µM ctDNA. All solutions were prepared in 80mM HEPES, 25 mM NaCl, 5% DMSO. Control wells contained EtBr and ctDNA at equivalent concentration to the test. Blank wells contained EtBr only in the same buffer. Fluorescence intensity due to DNA / EtBr binding was calculated using equation 1.

$$1) F = (F_s - F_b)/(F_c - F_b)$$

Where F is the (fractional) normalised intensity of fluorescence due DNA-bound EtBr. F_s is the observed fluorescence of the sample well, F_b is the fluorescence of the blank well and F_c is the fluorescence observed in the control well. Experiments conducted with Hoechst 34580 and Methyl green were conducted under equivalent conditions but with 5 µM fluorophore. Data was collected on a TECAN[®] Spark microplate reader. Fluorescence quenching of methyl Green and Hoechst 34580 were conducted in an equivalent manner but with final fluorophore concentrations of 5 µM. Excitation emission wavelengths used were 530/590 nm for EtBr, 350/450 nm for Hoescht 34580 and 630/670 nm for MG.

Microscale Thermophoresis

Samples for MST analysis were prepared to contain 500nM F-DDH in 80 mM HEPES, 25 mM NaCl, 5% DMSO with Cu(II)-TC-Py at varying concentrations. MST power was set to medium and excitation power was set to automatic mode in the red channel, typical excitation power was approximately 14%. The laser-on time was set to 20 seconds and with data being recorded for two seconds prior to the laser being turned on and for 2 seconds post being turned off.

195 **Fluorescence Melting**

196 Thermal melting analysis was performed on a Roche LightCycler®480 II using 80mM HEPES 25mM
197 NaCl buffer. Prior to analysis FRET-DDH was denatured by heating to 90°C (10°C/min, 2 min hold) and
198 reannealed at 12°C(0.5°C/min, 20min hold). Sample tubes for analysis were prepared to contain 1 µM
199 FRET-DDH and Cu(II)-TC-Py at various r loadings. ($r = \text{Cu(II)-TC-Thio} / [\text{FRET-DDH}]$). Melting was
200 conducted in triplicate at a ramp rate of 0.5 °C min⁻¹ up to a maximum of 95°C. T_m values were taken as
201 the midpoint of the melting curves.

202

203 **Single Molecule Analysis – DNA Binding**

204 *Sample Preparation*

205 Samples for analysis were prepared to contain 5 µM (base pairs) of lambda DNA and 5 µM YOYO-1 with
206 varied concentrations of Cu(II)-TC-Py in a total volume of 10 µL and incubated for 30 minutes at room
207 temperature. Before imaging, 0.5 µL of β-mercapto ethanol was added to minimize YOYO-1 photocleav-
208 age and the sample was diluted to 50 µL to prevent overloading of nanochannels.

209 *DNA Stretching and Imaging*

210 Samples were added to nanofluidic chips that were fabricated as described elsewhere. Compressed air
211 was used to move DNA molecules from the sample well, into the microchannel and to accumulate at the
212 nanochannel interface. Air pressure was then increased manually to drive DNA molecules into nanochan-
213 nels where images were taken at the excitation and emission wavelengths of YOYO-1 with 2% excitation
214 laser intensity, collecting 20 frames at 100 millisecond exposure times each to give 2 second videos of
215 each imaging field.

216 *Data Processing*

217 Data analysis was performed with the freeware ImageJ and a custom-written MatLab based software.
218 For DNA confined in nanochannels a kymograph (timetrace) was extracted for each movie using ImageJ
219 and the average distance between either end of the DNA molecule and the average pixel intensity along
220 the DNA molecule was found using the custom MatLab software. For mapping, the initial alignment is
221 done on the center of the molecule to eliminate the effects of drift along the nanochannel. The intensity
222 profile from the molecule is fitted to a linear combination of error functions. A finer alignment procedure
223 is subsequently performed on distinct features (peaks or dips in intensity) along the DNA.

224 **Docking Studies**

225 Docking studies of Cu(II)-TC-Py with a B-DNA dodecamer (PDB: 1BNA) was performed using AutoDock
226 Vina.⁷ The Cu(II)-TC-Py was prepared by first removing nitrates from the DFT structure. Atomic charges
227 and rotatable bonds were then defined in Autodock tools (version 1.5.7) and the structure output file
228 saved in .pdbqt format. The DNA receptor was prepared by removing water molecules, building in miss-
229 ing hydrogen atoms, and assigning atomic charges. Grid boxes were sized to incorporate the entire DNA
230 fragment and 10 docking poses were tested and ranked in terms of stability using the scoring function in
231 AutoDock Vina

232

233 **Molecular Dynamics**

234 MD simulations were performed using the GROMACS-2018.4 code.^{8,9} The topology and parameters for
235 the DNA model were defined by the CHARMM36m classical mechanics force field.¹⁰ The topology and
236 parameters for Cu(II)-TC-Py were obtained from density functional theory (DFT) calculations using the

237 Gaussian 16 package followed by CHARMM-compatible charge fitting with Antechamber⁷ using Re-
238 strained Electrostatic Potential (RESP) calculations.¹¹
239 The Cu(II)-TC-Py-DNA complex was solvated in a large cuboid of TIP3P water molecules with counter-
240 ions added to balance any formal charge. 0.15 M NaCl was added to model physiological salt concen-
241 tration. Energy minimisation was followed by thermalisation and equilibration under constant volume
242 (NVT) and then constant pressure (NPT) conditions. Production MD simulations were carried out for 4
243 μ s for each complex, starting with PCU in the minor groove or PCU in the major groove, for a total of 8
244 μ s of free dynamics.

245 *Characterisation of interactions*

246 We performed the characterisation of interactions in Cu₃-TC-Py -DNA complexes by using the protein-
247 ligand interaction profiler (PLIP)¹², a web service for visualization and detection of non-covalent
248 (hydrogen bonds, metal complexes, hydrophobic interactions, stacking and salt bridge) binary contacts
249 in 3D complex structures. The analysis was carried out in two parts: first, for the full 4 μ s trajectory of
250 each system accounting for frames every 100 ns, and second, for the last 1 μ s of converged trajectory
251 accounting for frames every 1 ns.

252

253 **National Cancer Institute 60 Cell Line Screening (NCI-60)**

254 TC-1 (NSC: 843989), TC-Thio (NSC: 843990), and TC-Py (NSC: 843991) were submitted to the U.S.
255 National Cancer Institute (NCI) Developmental Therapeutics Program (DTP) for 60 human cancer cell
256 line screening. Growth inhibition (GI₅₀) data were identified using a five-dose exposure level and are
257 shown in **Table S3**. These results are categorised by cancer type across leukaemia, non-small cell lung
258 cancer, colon cancer, CNS cancer, melanoma, ovarian cancer, renal cancer, prostate cancer, and breast
259 cancer and visualised in a heat map using GraphPad Prism as shown in **Figure S23**.

260

261 **ICP-MS Studies of Intracellular Cu**

262 ICP-MS experiments were performed on MDA-MB-231 cells. An adequate number of cells were seeded
263 in a 150 mm diameter Petri dish using DMEM medium with 10% Fetal bovine serum and penicillin
264 streptomycin (100 unit/ml) and incubated in at 37 °C, 5% CO₂. When the cell confluency reached around
265 80–90%, a fresh medium containing 20 μ M of Cu(II)-TC-Py was added and incubated for 48 hours at 37
266 °C, 5% CO₂. Cells were harvested by trypsinization. The medium was removed by centrifugation, and
267 the cell pellet was washed twice with cold DPBS. The nucleus and DNA of treated cells were then isolated
268 using the standard kit protocols mentioned below. The exact number of cells was always counted using
269 the hemocytometer. All experiments were performed in duplicate.

270 Total cells: To determine the total copper uptake, 2×10^6 cells were collected and digested using 500 μ L
271 of 70% nitric acid at 65 °C for 12 h. 100 μ L of the acid solution was further diluted in 3000 μ L of MilliQ
272 water. Finally, the copper concentration was measured using ICP-MS. Each experiment was performed
273 in triplicate

274 Nuclei: The nuclei isolation kit, NE-PER nuclear and cytoplasmic extraction reagent (Thermo-scientific)
275 was used to isolate the nuclei from the complex-treated cells, and the standard kit protocol was employed
276 for the isolation process. 2×10^6 of the complex-treated cells were used to isolate the nuclei pellet using
277 the protocol. We followed the first step of the supplier protocol and we stopped at the nuclear pellet step.
278 Then, nuclear pellet is dissolved in 500 μ L of 70% nitric acid at 65 °C for 12 h.

279

Bacterial Assays

Bacterial growth conditions and compounds preparation

Unless stated otherwise, *Bacillus subtilis* strains were aerobically grown in Mueller Hinton Broth (MHB). All tested compounds except for ciprofloxacin were dissolved and diluted in DMSO. Ciprofloxacin was dissolved and diluted in water. Unless stated otherwise, all assays were performed in biological triplicates. Minimal inhibitory concentrations (MICs) were determined in a broth microdilution assay according to Clinical and Laboratory Standards Institute (CLSI) guidelines. The MIC was defined as the lowest concentration inhibiting growth of a 5×10^5 colony forming units (CFU)/mL inoculum after a 16-h incubation period at 37 °C.

Bacterial cytological profiling (BCP)

Bacterial cytological profiling was performed as described by Wenzel *et al.*¹³ In short, *B. subtilis* UG10 (*trpC2 amyE::Pxyl-recA-mgfp*) was grown in Muller Hinton Broth (MHB) supplemented with 0.1% (w/v) xylose at 30 °C. After reaching an OD₆₀₀ of 0.3, cells were treated with 0.5× and 1× MIC of the respective compounds for 10 and 30 min. Ciprofloxacin and nitrofurantoin were used as positive controls. Immediately prior to imaging, cells were stained with 1 µg/mL of the DNA dye DAPI for 5 min. Samples (0.5 µL) were spotted on glass slides covered with a thin film of 1.2% agarose, covered with a poly-L-dopamine-coated coverslip,¹⁴ and imaged using a Nikon Eclipse Ti2 inverted fluorescence microscope equipped with a CFI Plan Apochromat objective (DM Lambda 100X Oil N.A. 1.45, W.D. 0.13mm, Ph3), a Lumencor Sola SE II FISH 365 light source, a Photometrics PRIME BSI camera, an Okolab incubator, and NIS ELEMENTS AR 5.21.03 software.

BCP image analysis

Images were processed and analyzed with Fiji and the ImageJ plugin MicrobeJ.^{15,16} The MicrobeJ parameters for bacterial detection in the phase contrast were set to smoothed segmentation with an area of 1 µm²-max. The width and circularity were adjusted accordingly to ensure proper detection while other parameters remained at default settings. All chained cells were assessed and separated using the MicrobeJ manual editing interface.¹⁶ For DNA compaction analysis, the maxima of foci detection were used as described previously.¹⁷ The parameters within the maxima detection remained at default settings. The Z-score and tolerance were adjusted manually to ensure fitting DNA detection. The compaction was calculated based on the quotient of the cell area divided by the DNA area. To quantify RecA-GFP foci, the total number of cells showing the foci and the total number of analysed cells were counted manually. All unfocused and visibly lysed cells were excluded from the analysis. P values were calculated using either heteroscedastic or nested t-tests, as specified in the figure legends, using OriginPro (OriginLab Corporation version 2023) or GraphPad Prism.

Bacterial chromosomal DNA preparation

Overnight cultures of *B. subtilis* 168CA¹⁸ were diluted in 20 mL MHB and grown at 30 °C until reaching an OD₆₀₀ of 0.3. Cells were then split and treated with either 64 µg/mL nitrofurantoin, 0.75 mM AG1, or left untreated as control. After 30 min of treatment, chromosomal DNA was isolated from all samples following a standard phenol-chloroform protocol.¹⁹ DNA was quantified using a Qubit 4 fluorometer following the protocol of the dsDNA Broad Range Assay kit (Invitrogen, Thermo Fisher, USA). Wide bore pipette tips were used throughout the experiment to minimize shear-induced fragmentation of the DNA.

Pulse field gel electrophoresis (PFGE)

Isolated DNA was separated in 20-50 kb resolution by PFGE using a 1% agarose gel run in a CHEF III DR System (Bio-Rad Laboratories, Hercules, CA, United States) with 0.5× TBE (45 mM Tris-HCl, pH 8.0; 45 mM boric acid; 1 mM EDTA) as running buffer. Electrophoresis was performed for 24 h at 14 °C. The forward and reverse voltages were 9 and 6 V/cm, respectively, with an initial switch time of 0.86 s

326 and final switch time of 0.92 s, with a 180° angle. The gel was stained with 1× concentrated SYBR Safe
327 DNA gel stain (Invitrogen) for at least 30 min before imaging in a UV transilluminator with default auto
328 optimal exposure settings for 590/110 SYBR safe gels (BioRad ChemiDoc MP imaging system, Im-
329 ageLab Touch software v 2.3.0.07).

330

331 **Bacterial DNA fluorescence microscopy**

332 *Silanization of coverslips*

333 Stretching of DNA was performed on silanized glass coverslips. The silanization was done as follows:
334 18 × 18 mm coverslips were placed in a coverslip rack and carefully submerged in a mixture of 1% (3-
335 aminopropyl)triethoxysilane (Sigma Aldrich) and 1% allyltrimethoxysilane (Sigma Aldrich) in acetone so-
336 lution, and silanized overnight. The activated coverslips were rinsed with acetone:water solution (2:1
337 v/v) and dried under a nitrogen gas flow immediately before DNA stretching.

338 *DNA staining, stretching and imaging*

339 100 ng DNA were stained with 320 nM YOYO-1 (Invitrogen) in 0.5× TBE and supplemented with 2% β-
340 mercaptoethanol (BME, Sigma Aldrich) in a final volume of 50 μL. 3.2 μL of stained DNA sample were
341 placed at the interface of the silanized coverslip and a clean microscopy slide (VWR), causing the capil-
342 lary force between the silanized coverslip and the microscope slide to stretch the DNA. Extended DNA
343 molecules were visualized using a Zeiss Observer.Z1 fluorescence microscope equipped with an Andor
344 iXON Ultra EMCCD camera and a Colibri 7 LED illumination system. For imaging YOYO-1, band-pass
345 excitation filters (475/40 nm) and band-pass emission filters (530/50 nm) were utilized.

346 *Data analysis*

347 A custom-made MATLAB software was used to analyse DNA fragments. Stretched DNA molecules were
348 detected and the length of each molecule was measured in microns. The software was set to exclude
349 overlapping DNA strands from the analysis. One-way ANOVA statistical significance was determined
350 using Tukey's model for multiple comparisons with a confidence level of 95%. P-values are represented
351 using the GraphPad PRISM style; ****P < 0.0001. The distribution graph was created in OriginPro
352 (OriginLab Corporation version 2023).

353

354 **DNA Cleavage by Agarose Gel Electrophoresis**

355 Cleavage reactions were prepared to a final volume of 20 μL in 100 μL Eppendorf tubes and contained
356 400ng supercoiled pUC19 DNA, 1 mM Na-L-ascorbate (where indicated) and 25 mM NaCl in 80 mM
357 HEPES buffer (pH = 7.4). Cleavage reactions with ROS scavengers were prepared to contain 10 mM of
358 the ROS scavenger by addition of 1 μL of a 200 mM stock solution prior to DNA addition. Reactions
359 probing the cleavage site were prepared by preparing reaction mixtures to contain 16 μM and 8 μM
360 methyl green and netropsin respectively from stock solutions prepared in 80 mM HEPES buffer (pH =
361 7.4). Upon addition of pUC19 the samples were incubated for 30 minutes at 37 °C, quenched with 6X
362 loading dye (Thermo Fisher R0611) and loaded on to a 1.3 % agarose gel, prepared using 1 X TAE
363 buffer and run at 70v for 90 minutes.

364

365 **Repair Assisted Damage Detection**

366 The protocol was adapted from Singh et al.^{20,21} The use of blood samples was approved by the Regional
367 Ethical Review Board in Gothenburg (Dnr: 246-07 and Dnr: 308-08).

369 *Blood Sample Collection*

370 Samples were collected from individuals with normal blood count from the Hematology Lab at the Clinical
371 Chemistry Department at Sahlgrenska University Hospital, Gothenburg, Sweden Lymphoprep (Axis-
372 Shield PoC AS, Oslo, Norway) was used to harvest peripheral blood mononuclear cells (PBMCs) via
373 density gradient-based separation. The blood-based study was performed with mixed blood samples
374 collected from different individuals and pooled together.

375 *Treatment of PBMCs with Cu(II)-TC-Py and antioxidants*

376 5×10^5 PBMCs were treated with 200 μ M Cu(II)-TC-Py and incubated for 2 h on a thermal block at 37°C.
377 For antioxidant-treated samples, PBMCs were pretreated with 1 mM of tiron, L-histidine, L-Methionine,
378 D-mannitol, and sodium pyruvate for 2 h prior to Cu(II)-TC-Py treatment.

379 *Extraction of DNA*

380 DNA was extracted using GenElute-Mammalian Genomic DNA Miniprep Kit (Sigma-Aldrich) following
381 manufacturer's instructions, after drug treatment and free radical scavenger incubation. DNA concentra-
382 tions were quantified using a NanoDrop 1000 spectrophotometer. Care was taken to avoid excess shear-
383 ing of DNA by using wide-bore tips.

384 *Fluorescent labeling of Cu₃-TC-Py induced DNA damage*

385 DNA (100 ng) was incubated with Endo III (2.5 U), Endo IV (2.5 U), Endo VIII (2.5 U), APE1(2.5 U), Fpg
386 (2.5 U) and AAG (2.5 U) in 1× CutSmart Buffer for 1 h at 37°C for *in vitro* DNA repair initiation. dNTPs
387 (1 μ M of dATP, dGTP, dCTP, 0.25 μ M dTTP and 0.25 μ M aminoallyl-dUTP-ATTO-647N) were incorporated
388 at the damage sites in 1× NEBuffer 2 using DNA polymerase I (1.25 U) at 20°C. Subsequently, the reac-
389 tion was terminated with 2.5 μ l of 0.25 M EDTA.

390 *Salinization of coverslips*

391 18 × 18 mm glass coverslips (Thermo Fischer Scientific) were placed in a coverslip rack and carefully
392 put into an acetone solution containing 1% (3-aminopropyl) triethoxysilane (APTES) and 1% allyltri-
393 methoxysilane (ATMS) (v/v) and coated overnight.²² Coated coverslips were rinsed with acetone:water
394 solution (2:1 v/v) to remove residues for reproducible stretching of DNA. The slides were always used on
395 the day they were produced.

396 *Stretching of DNA and imaging*

397 The Aminoallyl-dUTP-ATTO-647N incorporated fluorescent DNA samples were diluted with 0.5× TBE
398 and stained with 320 nM YOYO-1 (Invitrogen) in a total volume of 50 μ l. β -mercaptoethanol (2% v/v,
399 Sigma-Aldrich) was added prior to image acquisition to minimize photodamage. The DNA samples were
400 stretched by placing 3.2 μ l at the interface of the silane-activated coverslip and a microscopy slide (VWR
401 Frosted). Zeiss Observer.Z1, equipped with an Andor iXON Ultra EMCCD camera and a Colibri 7 LED
402 illumination system was used to obtain the fluorescence images of the stretched DNA molecules. Each
403 image consisted of two colours, YOYO-1 (green channel), and aminoallyl-dUTP-ATTO-647N (red chan-
404 nel) having appropriate band-pass excitation filters (475/40 and 640/30 nm) and bandpass emission
405 filters (530/50 and 690/50 nm).

406

Software analysis

A custom-made MATLAB script was used to analyse the data which estimates the length of the stretched DNA molecule in micron (μm) and counts the total number of Aminoallyl-dUTP-ATTO-647N dots along the DNA. The results were expressed as Dots.MBp⁻¹ by stretching lambda DNA (48502 bp, New England Biolabs) in a similar buffered conditions to determine 1 μm stretched DNA to be ~3000 bp. DNA molecules that overlapped as wells as dots at the end of the DNA molecule which could have resulted from DNA strand breaks during the DNA extraction process were excluded from the analysis.

Statistics

Experiments were conducted in technical duplicates and analyzed using GraphPad Prism. Statistical significance was evaluated with one-way ANOVA, and p-values are presented in the GraphPad Prism format: ns (not significant) ****P <0.0001

423

424

425

426

427

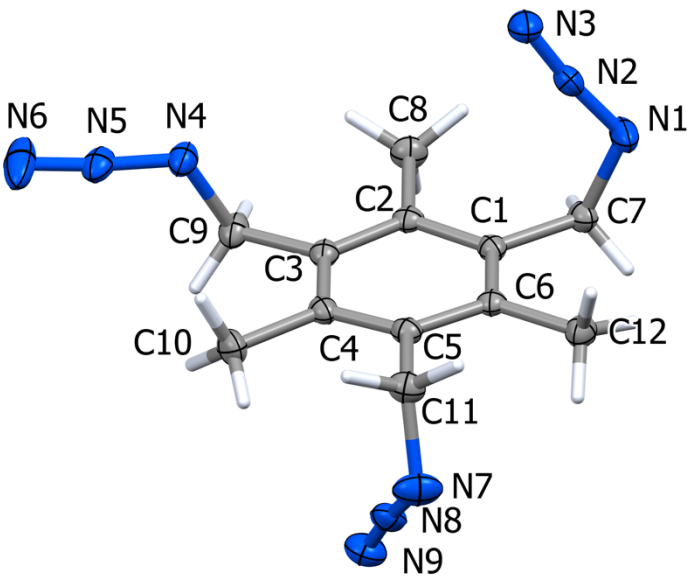


Figure S1: Crystal structure of Triazide showing 50% probability atomic displacement ellipsoids

Table S1: Crystal data and structure refinement Triazide

CCDC code	2409062
Empirical formula	C ₁₂ H ₁₅ N ₉
Formula weight	285.33
Temperature/K	100.00(10)
Crystal system	monoclinic
Space group	P2 ₁ /c
a/Å	12.80290(10)
b/Å	10.80650(10)
c/Å	10.06400(10)
α/°	90
β/°	90.7580(10)
γ/°	90
Volume/Å ³	1392.28(2)
Z	4
ρ _{calc} g/cm ³	1.361
μ/mm ⁻¹	0.760
F(000)	600.0
Crystal size/mm ³	0.17 × 0.07 × 0.06
Radiation	Cu Kα (λ = 1.54184)

2 θ range for data collection/ $^{\circ}$	6.904 to 148.86
Reflections collected	39527
Independent reflections	2838 [$R_{\text{int}} = 0.0236$, $R_{\text{sigma}} = 0.0087$]
Data/restraints/parameters	2838/0/193
Goodness-of-fit on F^2	1.034
Final R indexes [$I \geq 2\sigma(I)$]	$R_1 = 0.0352$, $wR_2 = 0.0940$
Final R indexes [all data]	$R_1 = 0.0376$, $wR_2 = 0.0963$
Largest diff. peak/hole / $e \text{ \AA}^{-3}$	0.25/-0.24

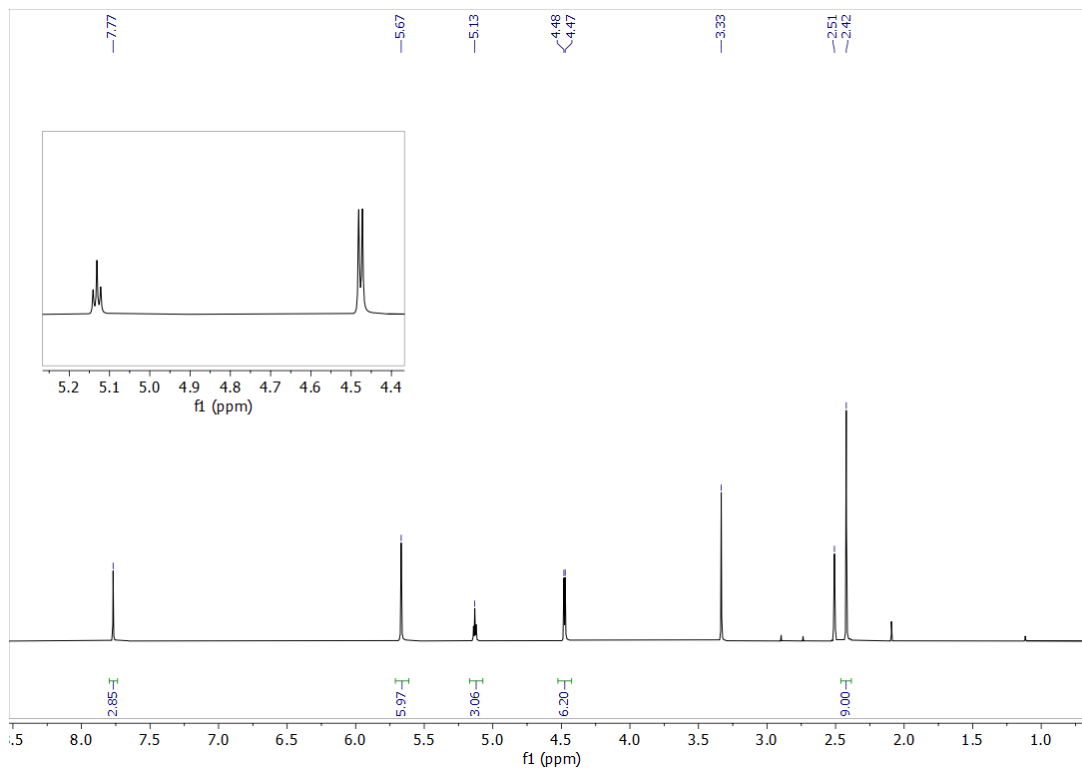


Figure S2: ^1H NMR Spectra of TC-OH in DMSO-d_6 600 MHz

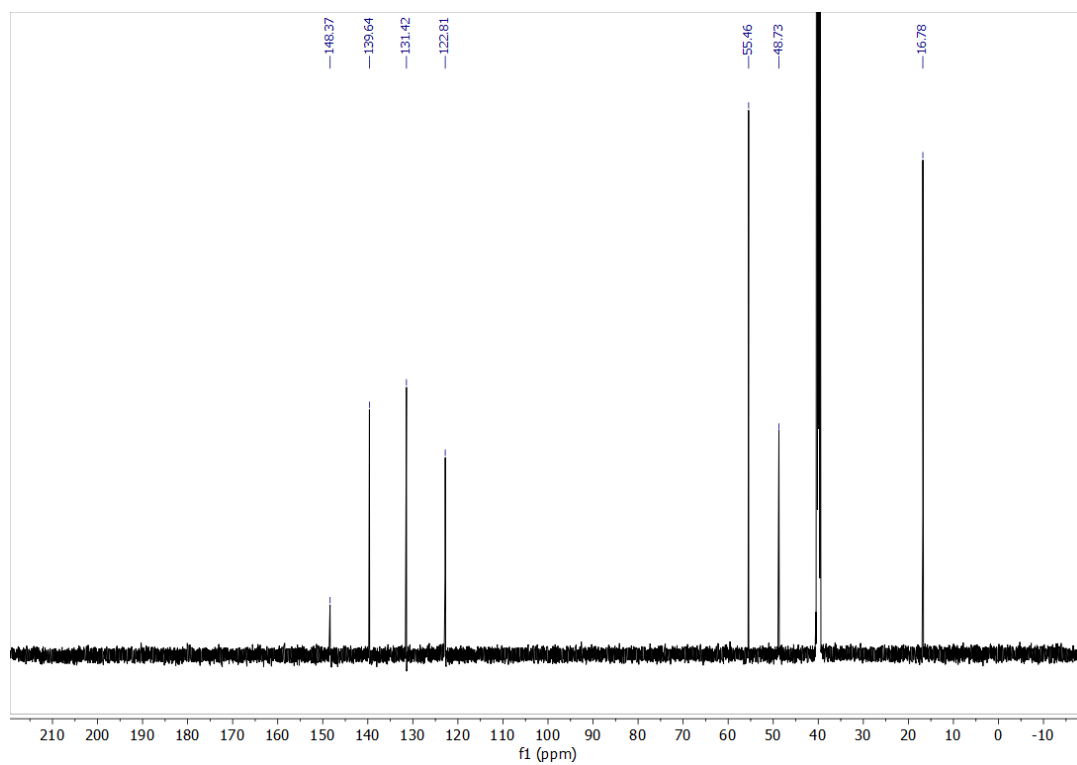


Figure S3: ^{13}C NMR of TC-OH

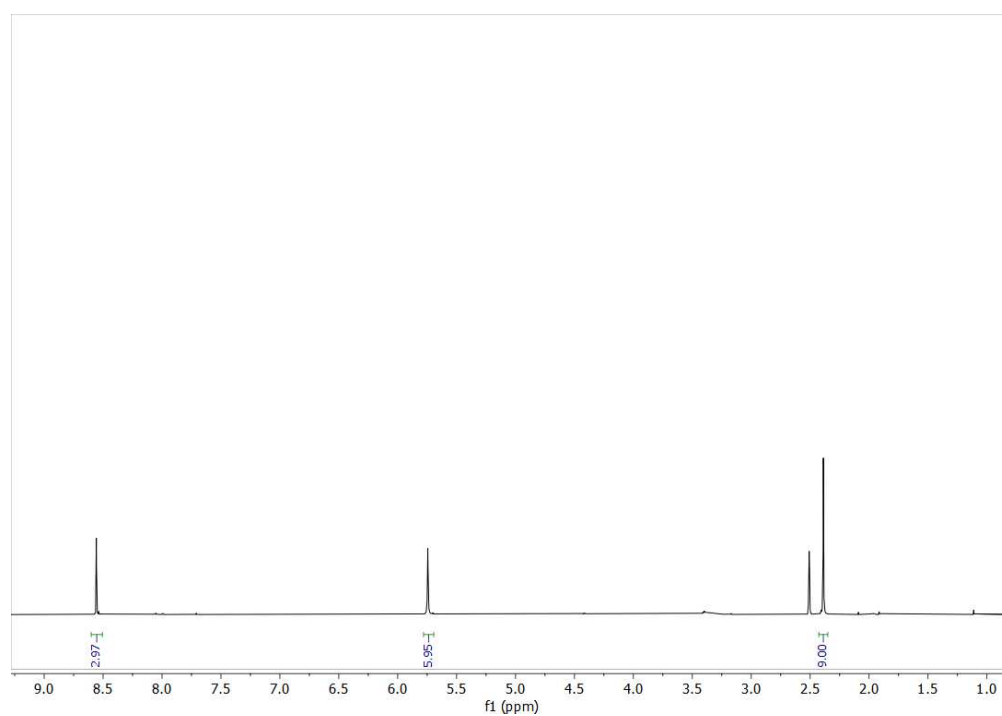


Figure S4: ^1H NMR Spectra of TC-Acid in DMSO-d_6 600MHZ

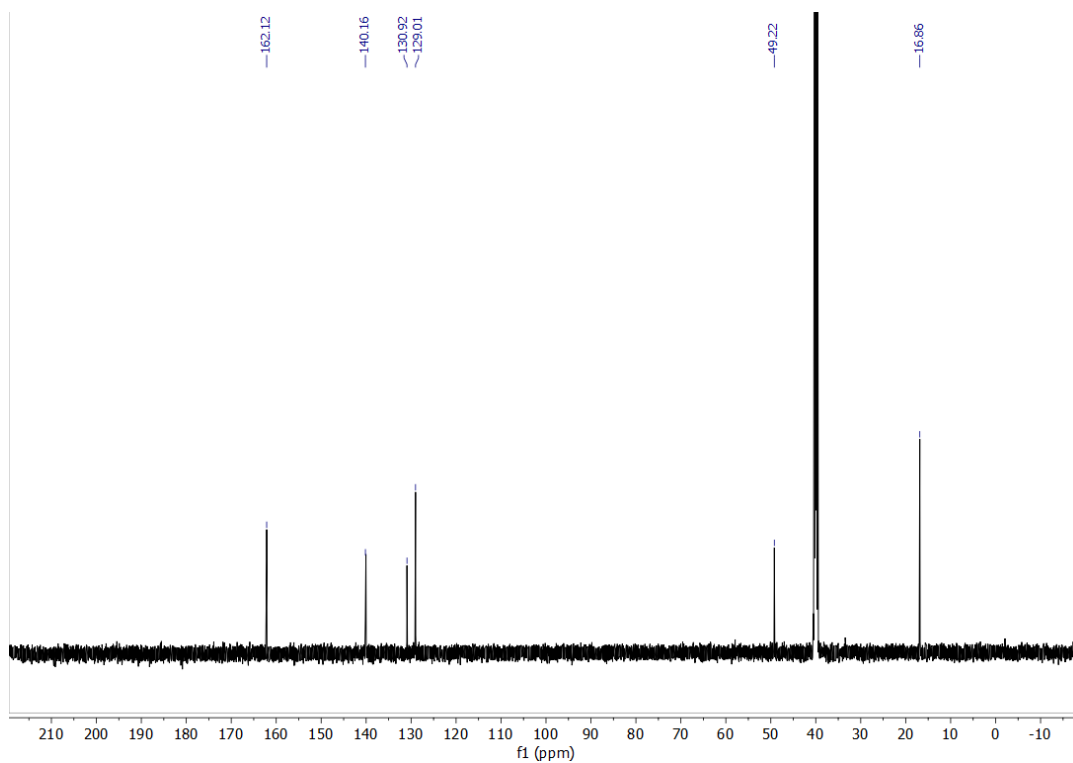


Figure S5: ^{13}C NMR of TC-ACID in DMSO- d_6

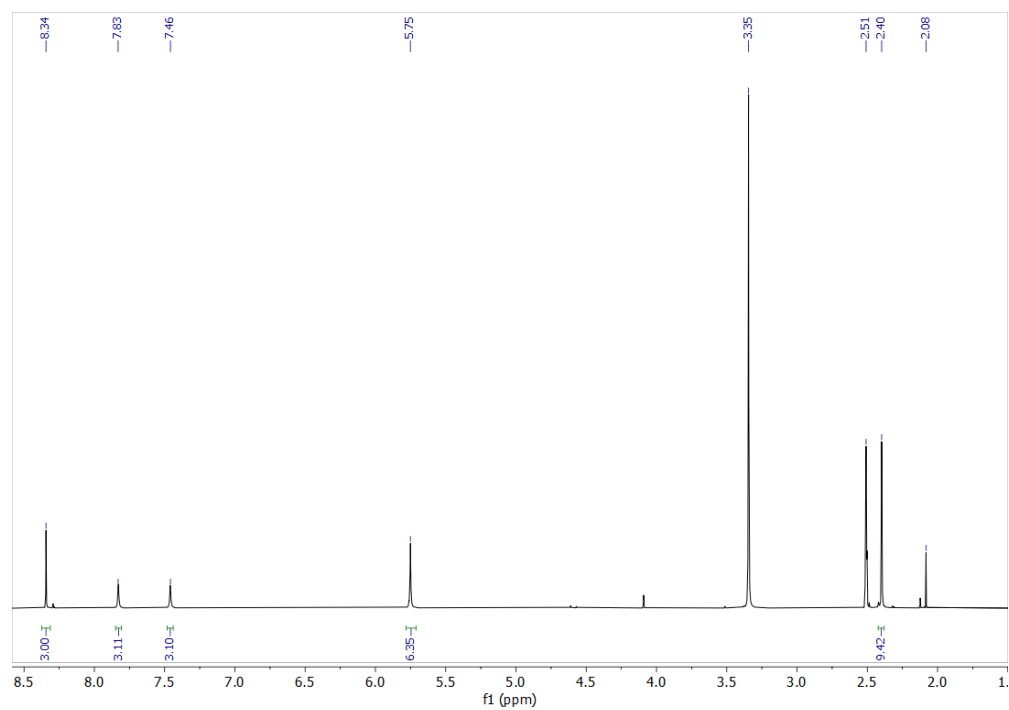


Figure S6: ^1H NMR of TC-Amide in DMSO- d_6

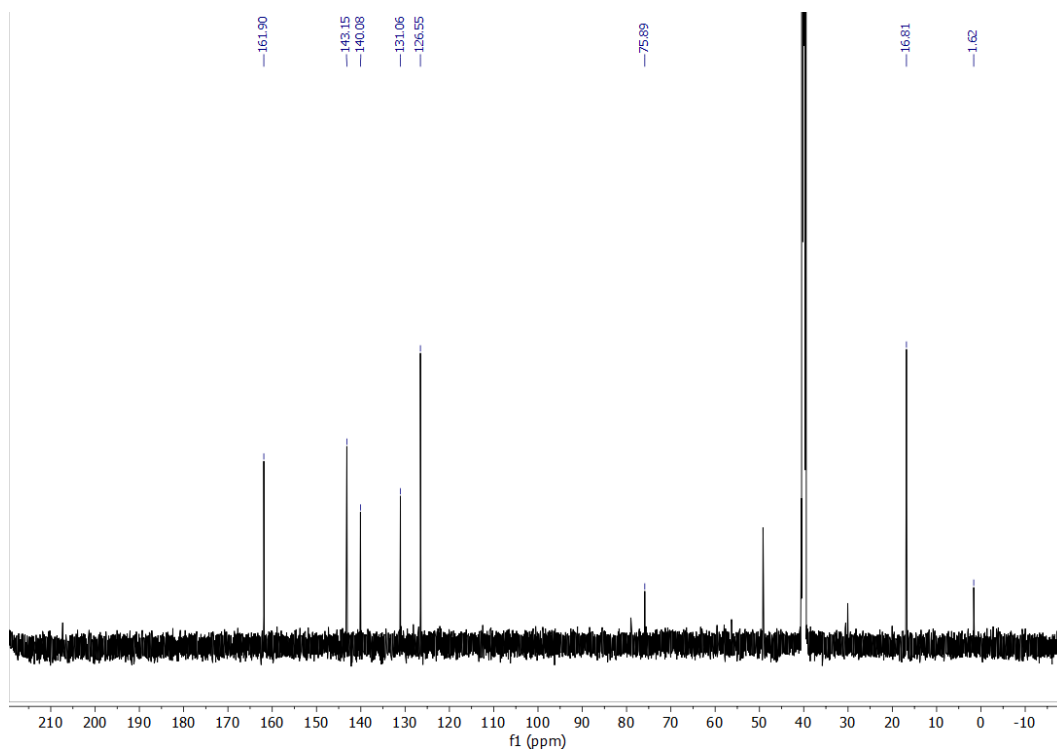


Figure S7: ^{13}C NMR of TC-Amide in DMSO- d_6

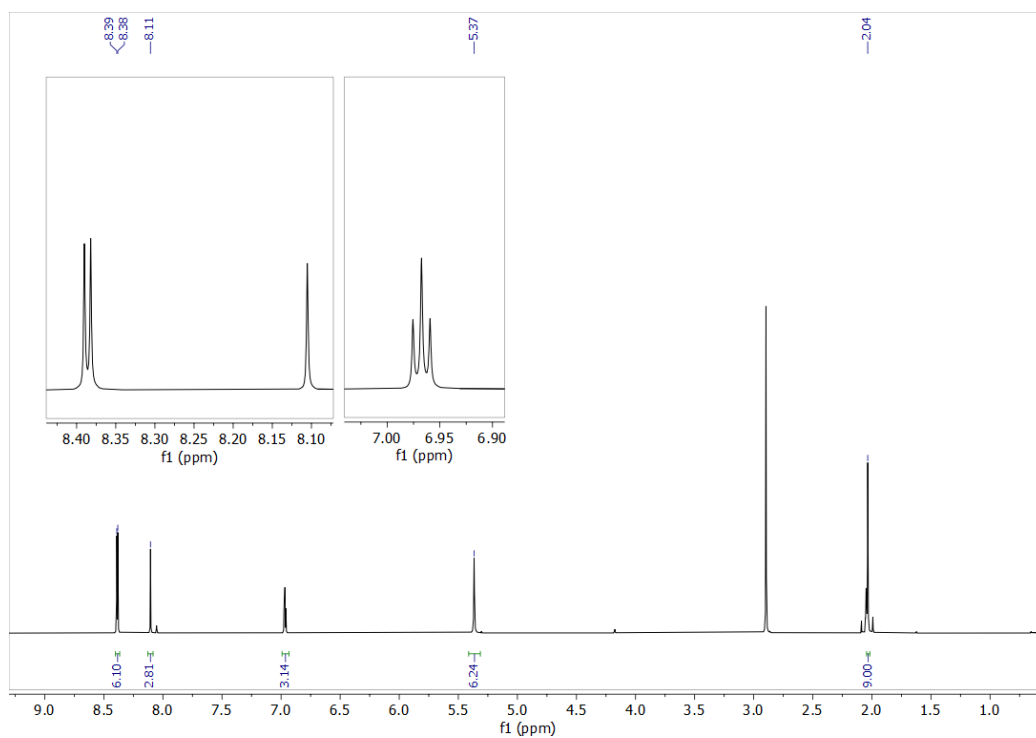


Figure S8: ^1H NMR Spectra of TC-Pym in DMSO- d_6 600MHz

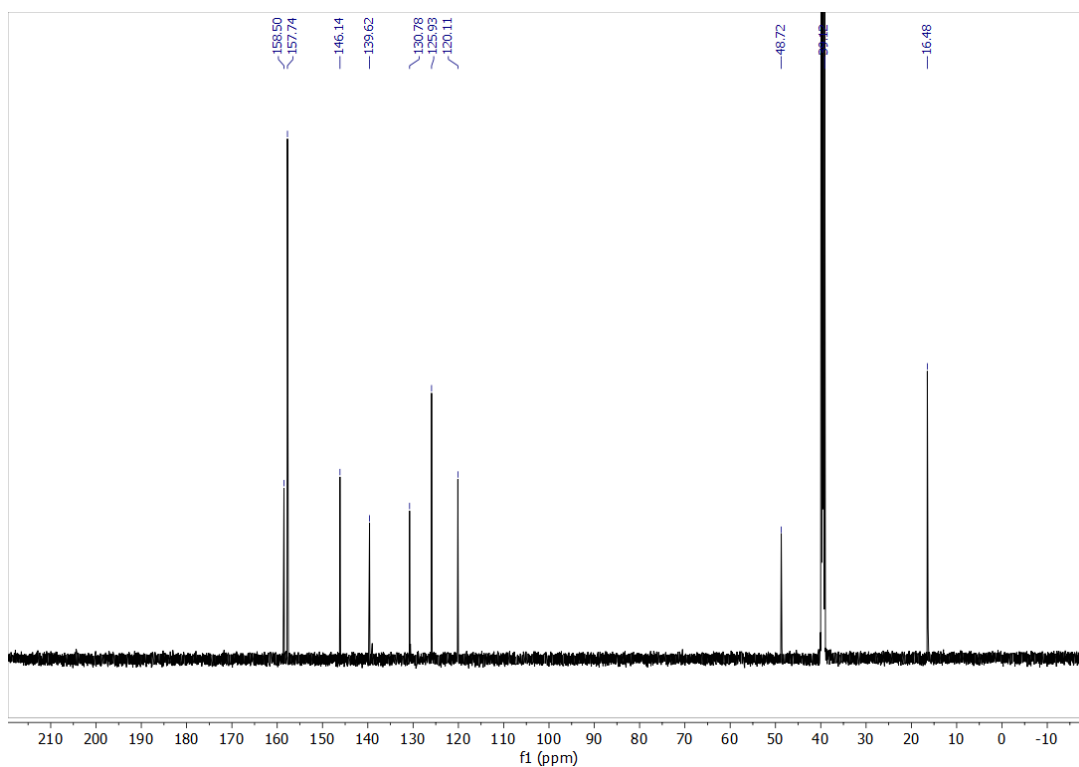


Figure S9: ¹³C NMR of TC-Amide in DMSO-d₆

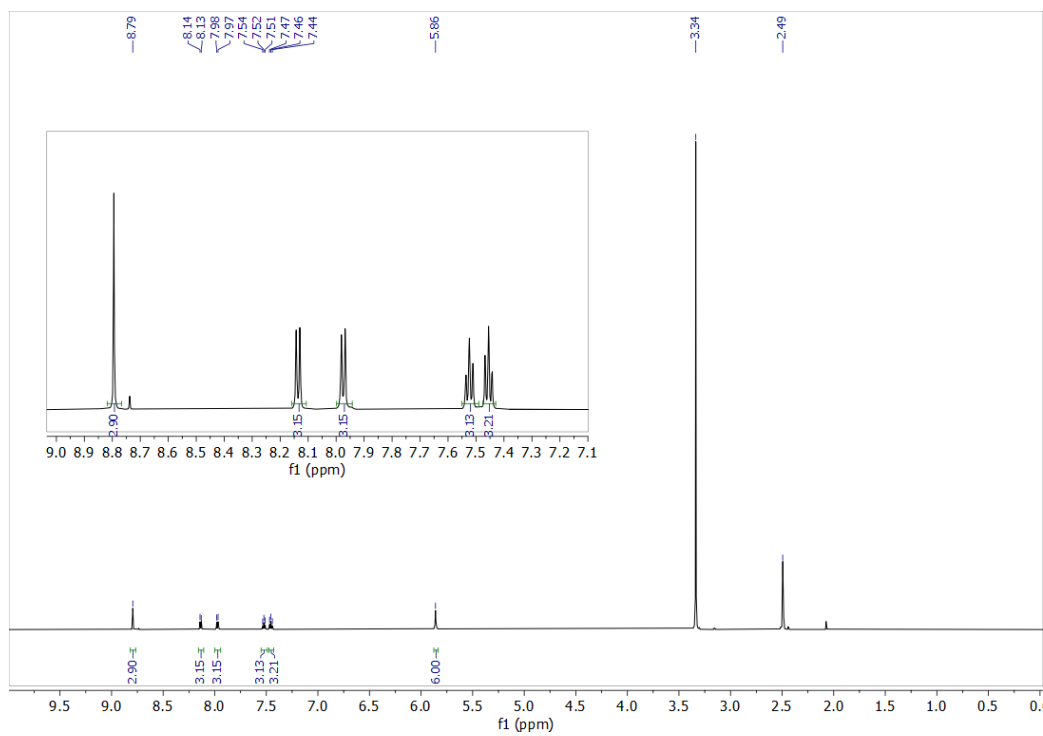
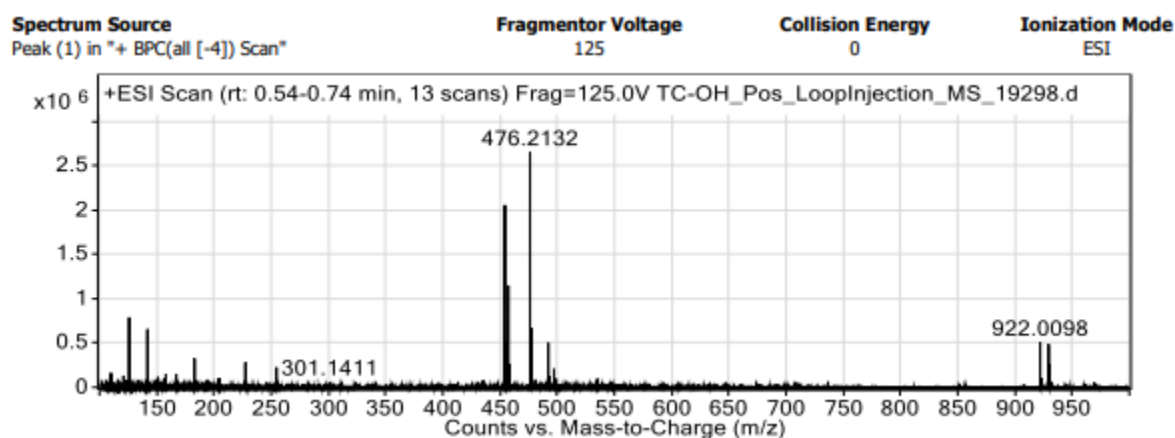


Figure S10: ¹H NMR of TC-Benzo in DMSO-d₆ 600 MHz

457

458

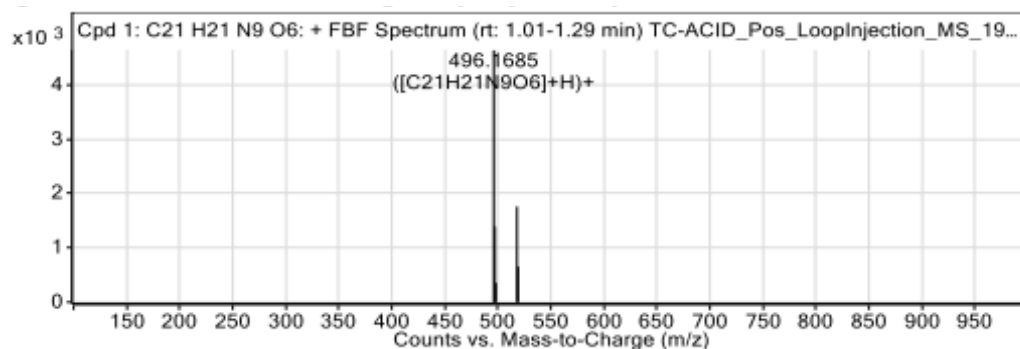


459

460

461

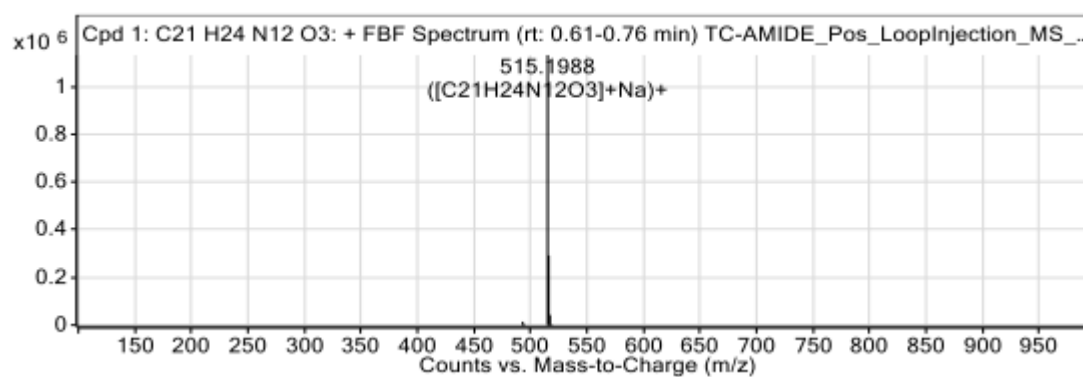
Figure S11: ESI-MS spectrum of TC-OH in positive ionization mode



462

463

Figure S12: ESI-MS spectrum of TC-Acid in positive ionization mode



464

465

Figure S13: ESI-MS spectrum of TC-Amide in positive ionization mode.

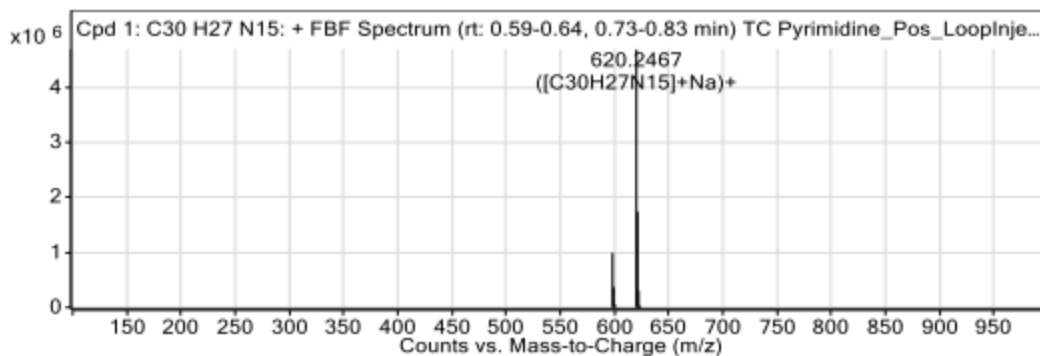


Figure S14: ESI-MS spectrum of TC-Pyrm in positive ionization mode

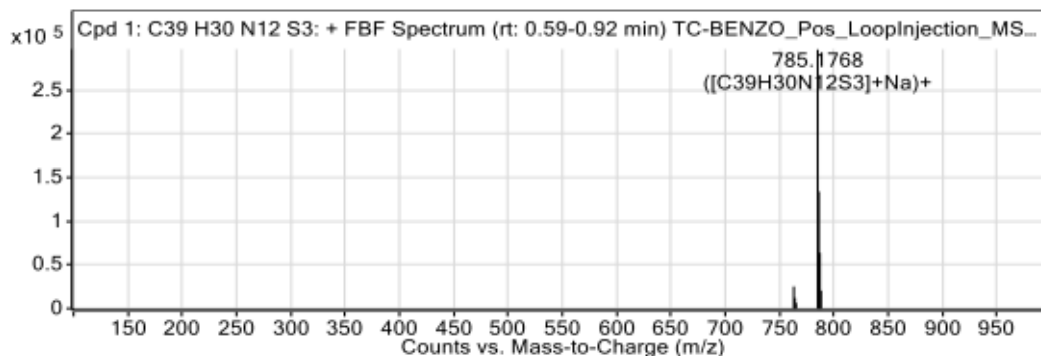


Figure S15: ESI-MS spectrum of TC-Benzo in positive ionization mode

Table S2: TC-Cu species identified by ESI-MS. Listed are molecular and elemental formulae with corresponding expected and found monoisotopic m/z values.

Complex / adduct (Formula)	Expected m/z	Found m/z
TC-Py + 3Cu		
$[\text{Cu}_3(\text{TC-Py})(\text{NO}_3)_5]^+$ ($\text{C}_{33}\text{H}_{30}\text{Cu}_3\text{N}_{17}\text{O}_{15}$)	1092.99	1092.98
$[\text{Cu}_3(\text{TC-Py})(\text{NO}_3)_4]^{2+}$ ($\text{C}_{33}\text{H}_{30}\text{Cu}_3\text{N}_{16}\text{O}_{12}$)	515.50	515.50
$[\text{Cu}_3(\text{TC-Py})(\text{NO}_3)_6+\text{H}]^+$ ($\text{C}_{33}\text{H}_{31}\text{Cu}_3\text{N}_{19}\text{O}_{21}$)	1217.98	1217.91
$[\text{Cu}_3(\text{TC-Py})(\text{NO}_3)_6+\text{HNO}_3]^+$ ($\text{C}_{33}\text{H}_{31}\text{Cu}_3\text{N}_{20}\text{O}_{24}$)	1279.91	1279.88
TC-Pyrm + 3Cu		
$[\text{Cu}_3(\text{TC-Pyrm})(\text{NO}_3)_5]^+$ ($\text{C}_{30}\text{H}_{27}\text{Cu}_3\text{N}_{20}\text{O}_{15}$)	1095.98	1095.97
$[\text{Cu}_3(\text{TC-Pyrm})(\text{NO}_3)_4]^{2+}$ ($\text{C}_{30}\text{H}_{27}\text{Cu}_3\text{N}_{19}\text{O}_{12}$)	517.00	516.99
$[\text{Cu}_3(\text{TC-Pyrm})(\text{NO}_3)_6\text{Na}]^+$ ($\text{C}_{30}\text{H}_{27}\text{Cu}_3\text{N}_{21}\text{O}_{18}\text{Na}$)	1180.96	1180.94
$[\text{Cu}_2(\text{TC-Pyrm})(\text{NO}_3)_3]^+$ ($\text{C}_{30}\text{H}_{27}\text{Cu}_2\text{N}_{18}\text{O}_9$)	909.08	909.07

TC-Benzo + 3Cu		
$[\text{Cu}_3(\text{TC-Benzo})(\text{NO}_3)_5]^+$ ($\text{C}_{39}\text{H}_{30}\text{Cu}_3\text{N}_{17}\text{O}_{15}\text{S}_3$)	1260.91	1260.89
TC-OH + 3Cu		
$[\text{Cu}_3(\text{TC-OH})(\text{NO}_3)_5 \cdot 2\text{H} + 2\text{DMF}]^+$ ($\text{C}_{24}\text{H}_{32}\text{Cu}_3\text{N}_{15}\text{O}_{19}$)	1022.98	1022.91
$[\text{Cu}_3(\text{TC-OH})(\text{NO}_3)_2 \cdot 3\text{H}]^+$ ($\text{C}_{21}\text{H}_{24}\text{Cu}_3\text{N}_{11}\text{O}_9$)	762.96	762.96
TC-Acid + 3Cu		
$[\text{Cu}_3(\text{TC-ACID})(\text{NO}_3)_5 \cdot 2\text{H} + 2\text{DMF}]^+$ ($\text{C}_{27}\text{H}_{33}\text{Cu}_3\text{N}_{16}\text{O}_{23}$)	1137.97	1137.90
$[\text{Cu}_3(\text{TC-ACID})(\text{NO}_3)_5 \cdot 2\text{H} + 1\text{DMF}]^+$ ($\text{C}_{24}\text{H}_{26}\text{Cu}_3\text{N}_{15}\text{O}_{22}$)	1064.93	1064.85
$[\text{Cu}_3(\text{TC-ACID})(\text{NO}_3)_2 \cdot 3\text{H} + 1\text{DMF}]^+$ ($\text{C}_{24}\text{H}_{25}\text{Cu}_3\text{N}_{12}\text{O}_{13}$)	877.95	877.95

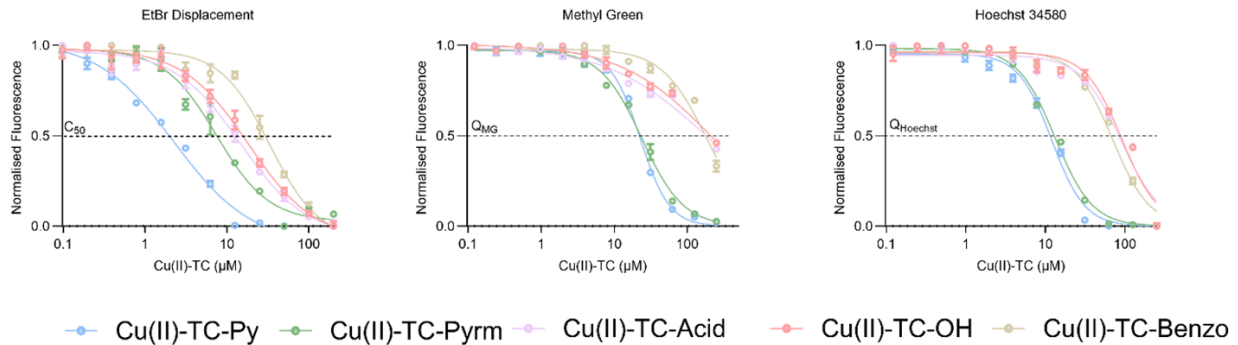


Figure S16: Fluorescence melting curves. Fluorophores indicated above each plot were kept constant while Cu-TC complexes were titrated. Plots were fit with nonlinear regression in Graphpad Prism to find C_{50} .

FDDH: 5'-**F**-CGCGAATTCGCGAAAAACGCGAATTCGCG-3'
 FRET-DDH: 5'-**F**-CGCGAATTCGCGAAAAACGCGAATTCGCG-**Q**-3'

Figure S17: Sequences of hairpins used for MST and fluorescence melting experiments. Loop region is highlighted grey. F = AlexaFluor 647, Q = Iowa Black.

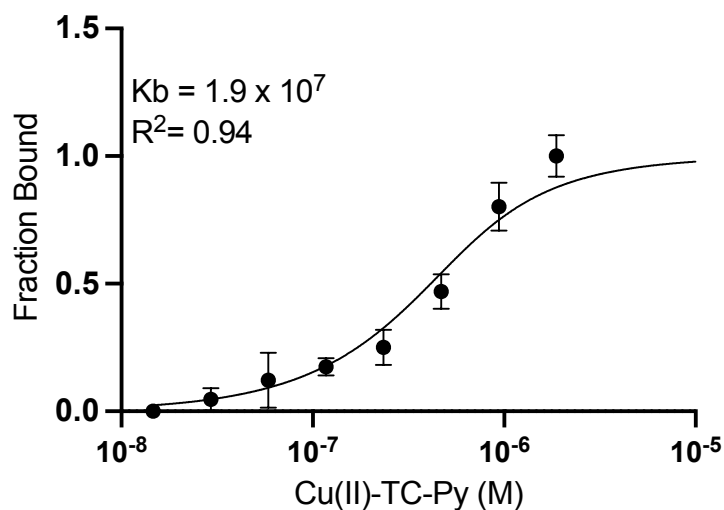


Figure S18: Fitting of the Bard equation to the binding region of MST data with n constrained to 2.

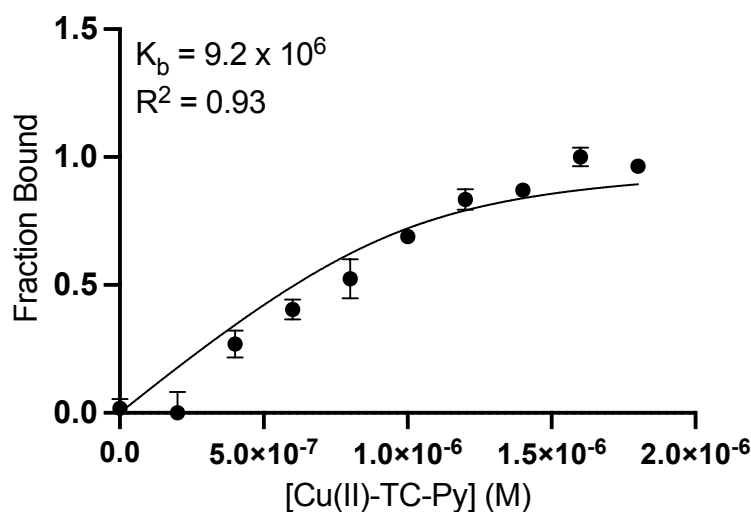


Figure S19: Fitting of the Bard equation to the binding region of thermal melting data with n constrained to 2.

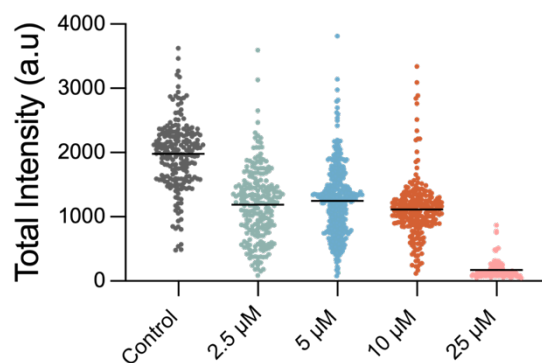
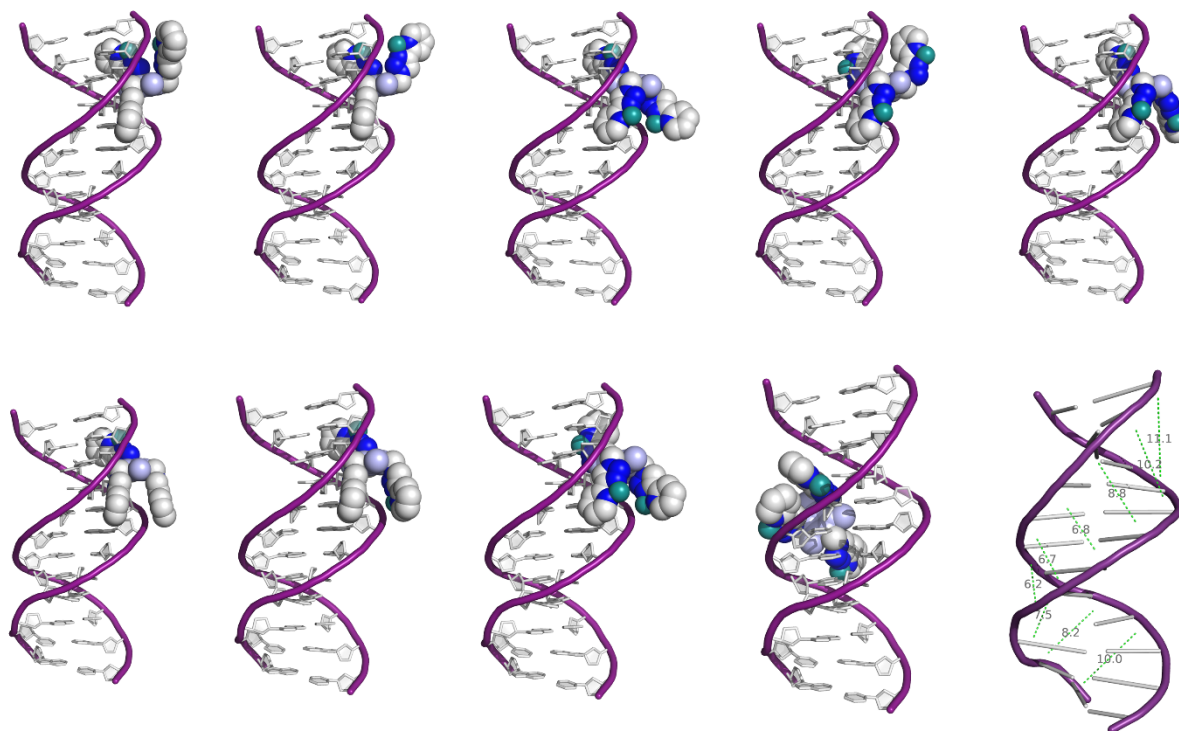


Figure S20: Plot of total fluorescence intensity observed along DNA molecules treated with 5 μ M YOYO and varying concentration of Cu₃-TC-Py

496

497



498

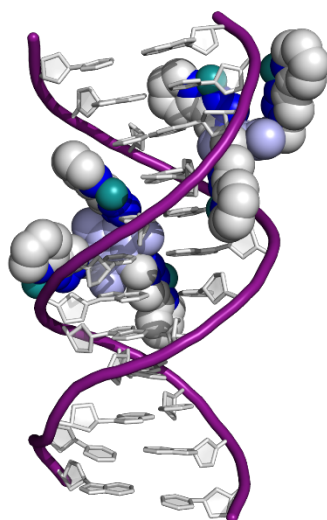
499

500

501

502

Figure S21: Nine output poses from docking studies of DNA (PDB: 1BNA) with modelled Cu(II)-TC-Pyr. Measurements of minor groove widths along the 1BNA structure, measured paths shown as dashed green lines.



503

504

505

506

507

Figure S22: Top ranked output from double docking experiment. Generated by using the top ranked pose from the original docking study, treated as a rigid structure, with an additional Cu(II)-TC-Py molecule.

508 **Table S3.** NCI-60 50% growth inhibition (GI₅₀) results of TC-Py and TC-Thio identified using the five-
509 dose response experimental results.

	<i>TC-Py</i>	<i>TC-Thio</i>
Cell line	GI₅₀ (μM)	GI₅₀ (μM)
CCRF-CEM	> 100	> 100
HL-60(TB)	> 100	> 100
K-562	> 100	> 100
MOLT-4	> 100	> 100
RPMI-8226	50.12	50.12
SR	93.33	93.33
A549/ATCC	30.20	79.43
EKVX	12.88	67.61
HOP-62	2.34	18.20
HOP-92	1.20	11.48
NCI-H226	3.09	22.91
NCI-H23	4.47	16.22
NCI-H322M	42.66	52.48
NCI-H460	24.55	50.12
NCI-H522	10.47	31.62
COLO 205	> 100	> 100
HCC-2998	28.18	> 100
HCT-116	7.41	20.89
HCT-15	77.62	> 100
HT29	> 100	> 100
KM12	> 100	> 100
SW-620	36.31	> 100
SF-268	6.61	22.91
SF-295	4.90	17.78

SF-539	2.95	15.85
SNB-19	3.72	19.05
SNB-75	2.24	11.48
U251	2.24	16.60
LOX IMVI	14.79	70.79
MALME-3M	19.05	10.96
M14	27.54	> 100
MDA-MB-435	58.88	> 100
SK-MEL-2	14.45	14.79
SK-MEL-28	56.23	> 100
SK-MEL-5	18.20	> 100
UACC-257	25.12	53.70
UACC-62	17.38	38.90
IGROV1	13.49	18.62
OVCAR-3	10.72	33.88
OVCAR-4	0.95	60.26
OVCAR-5	69.18	> 100
OVCAR-8	2.69	23.99
NCI/ADR-RES	12.02	36.31
SK-OV-3	3.16	14.79
786-0	2.88	19.05
A498	25.12	21.38
ACHN	21.38	25.70
CAKI-1	3.98	28.18
RXF 393	7.76	17.78
SN12C	12.02	33.11
TK-10	18.62	16.22
UO-31	13.80	> 100

PC-3	14.45	58.88
DU-145	27.54	52.48
MCF7	9.12	72.44
MDA-MB-231/ATCC	7.24	17.78
HS 578T	3.47	25.12
BT-549	12.59	15.49
T-47D	6.03	22.39
MDA-MB-468	10.72	20.42

510

511

512

513

514

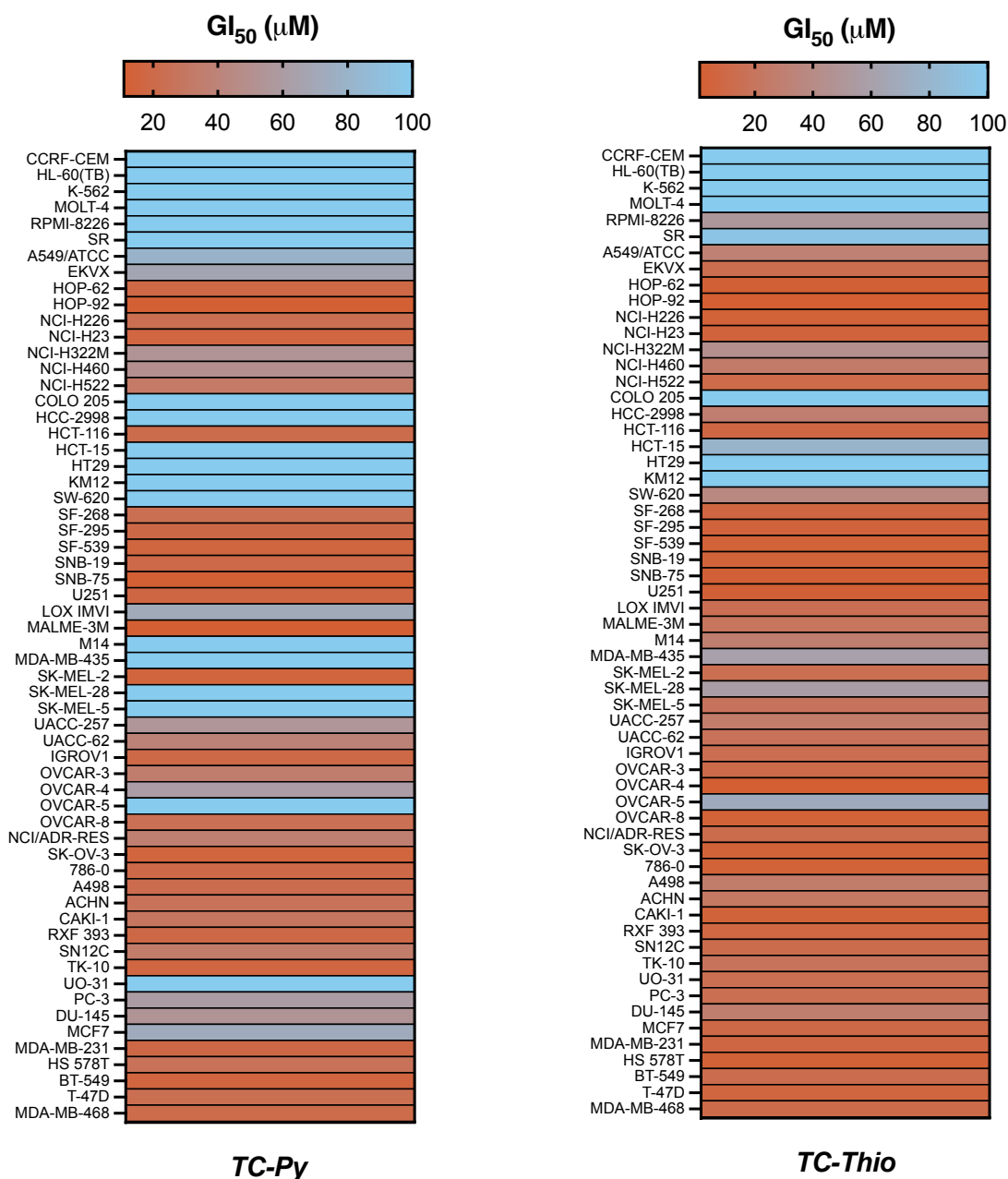
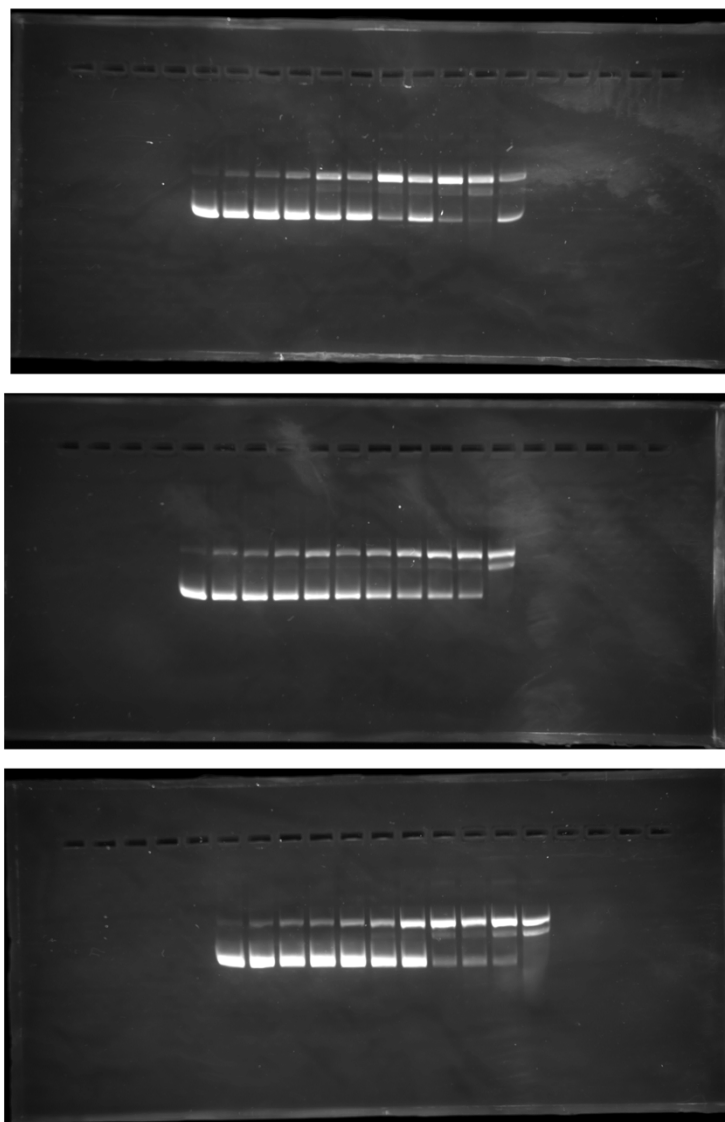


Figure S23. NCI-60 data for TC-Py and TC-Thio. Data presented as a heatmap showing 50% growth inhibition (GI_{50}) results arising from exposure of selected human cancer cell lines to the complex upon five-dose exposure.



519

520 **Figure S24:** Complete gels used for densitometry. All lanes contained 1mM Na-L-ascorbate, 400ng
 521 pUC19 DNA and 25mM NaCl in 80mM HEPES pH 7.2. Lanes 1-11 contained 0, 1, 2, 3, 4, 5, 6, 7, 8, 9,
 522 10 μ M Cu(II)-TC-Py respectively.

523

524

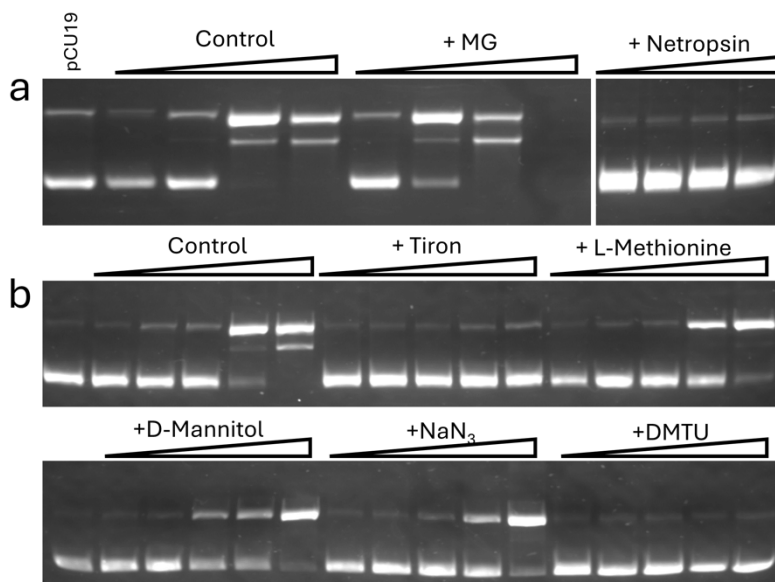


Figure S25: (a) Cleavage experiments in the presence of groove blocking agents, methyl green (16 μM) and netropsin (8 μM). Wedges above gels indicate increasing Cu₃-TC-Py concentrations of 4, 6, 8 and 10 μM. Lane 1 contained pUC19 DNA only. Control ramp contained pUC19 DNA and Cu₃-TC-Py only with no groove blocking agent. (b) DNA cleavage experiment in the presence of antioxidants (10mM). Each wedge indicates increasing Cu(II)-TC-Py concentration at 2, 4, 6, 8, 10 μM. Lane 1 contained pUC19 DNA only. The control gradient contained Cu₃-TC-Py and pUC19 with no antioxidant. All experiments contained 1mM Na-L-ascorbate.

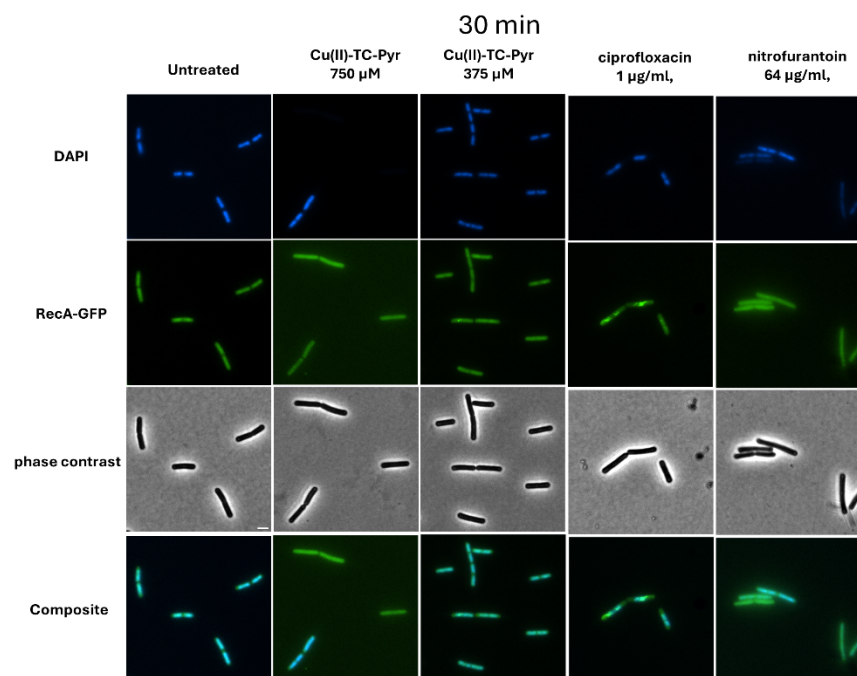
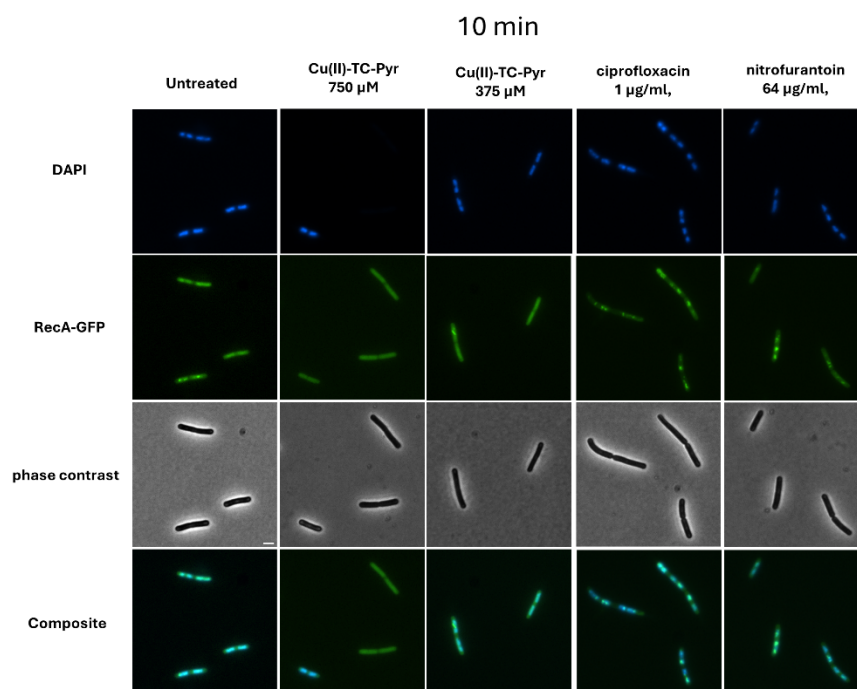


Figure S26: Microscopy images collected from bacterial cytological profiling experiments of cells treated with Cu₃-TC-Py ciprofloxacin or nitrofurantoin for 10 or 30 minutes. Cells contained a GFP-tagged Rec A and were stained with DAPI prior to imaging.

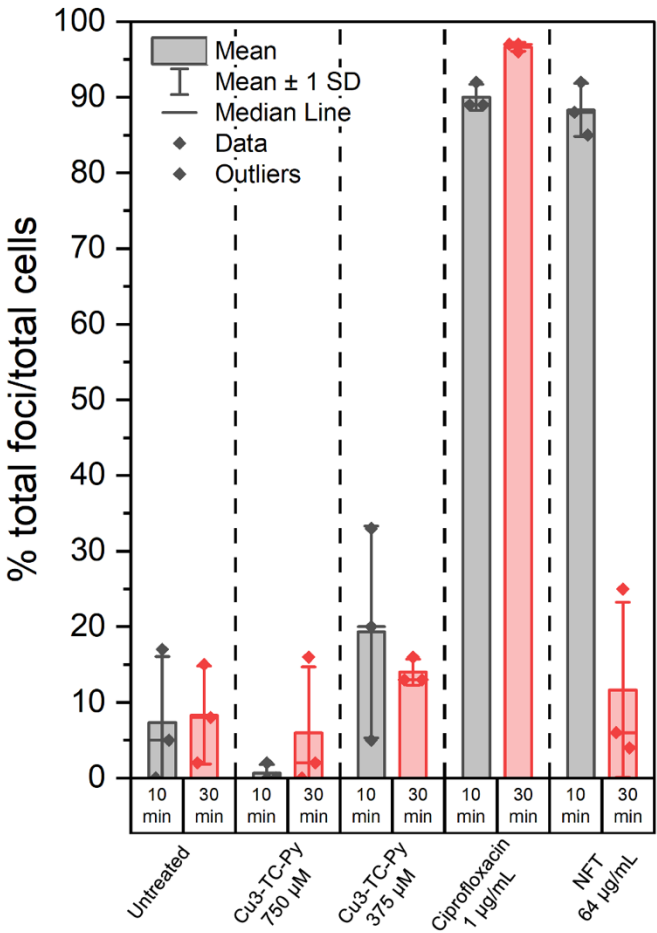


Figure S27: Quantification of RecA Foci in cells treated with varying Cu₃-TC-Py concentrations and fixed concentrations of ciprofloxacin and NFT.

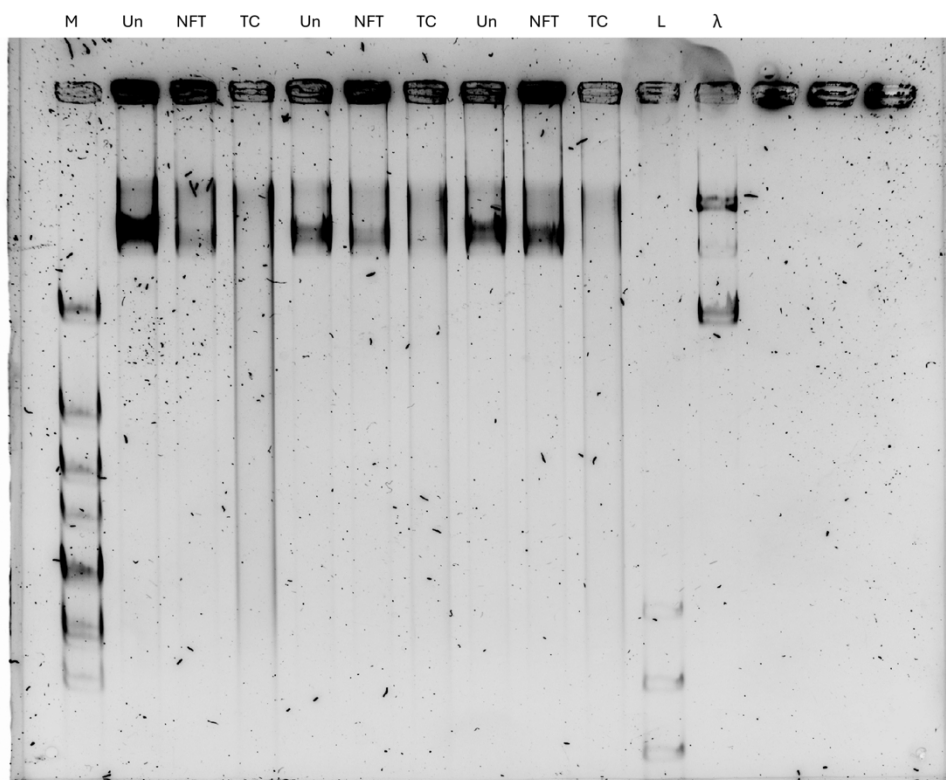


Figure S28: Pulse field electrophoresis. DNA was extracted from treated and untreated cells. Treated cells were incubated with 64 µg/mL (268 µM) nitrofurantoin (labelled NFT) or 750 µM Cu(II)-TC-Py (labelled TC) for 30 mins. Lane labelled M contained an NEB λ DNA monocut mix ladder, lane L contained GeneRuler 1 kb plus DNA ladder and the rightmost lane contained λ DNA as control for verifying accuracy of DNA ladders. Untreated samples are labelled Un.

568 **References:**

569

- 570 1 Rigaku Oxford Diffraction, CrysAlisPro version 1.171.43.115a (2024).
- 571 2 Hubschle, C. B., Sheldrick, G. M. & Dittrich, B. ShelXle: a Qt graphical user interface for
572 SHELXL. *J Appl Crystallogr* **44**, 1281-1284 (2011).
573 <https://doi.org/10.1107/S0021889811043202>
- 574 3 Dolomanov, O. V., Bourhis, L. J., Gildea, R. J., Howard, J. A. K. & Puschmann, H.
575 OLEX2: a complete structure solution, refinement and analysis program. *J Appl*
576 *Crystallogr* **42**, 339-341 (2009). <https://doi.org/10.1107/S0021889808042726>
- 577 4 Sheldrick, G. M. SHELXT - integrated space-group and crystal-structure determination.
578 *Acta Crystallogr A Found Adv* **71**, 3-8 (2015).
579 <https://doi.org/10.1107/S2053273314026370>
- 580 5 Sheldrick, G. M. Crystal structure refinement with SHELXL. *Acta Crystallogr C Struct*
581 *Chem* **71**, 3-8 (2015). <https://doi.org/10.1107/S2053229614024218>
- 582 6 McCann, M. *et al.* A new phenanthroline-oxazine ligand: synthesis, coordination
583 chemistry and atypical DNA binding interaction. *Chem Commun (Camb)* **49**, 2341-2343
584 (2013). <https://doi.org/10.1039/c3cc38710k>
- 585 7 Trott, O. & Olson, A. J. AutoDock Vina: improving the speed and accuracy of docking
586 with a new scoring function, efficient optimization, and multithreading. *J Comput Chem*
587 **31**, 455-461 (2010). <https://doi.org/10.1002/jcc.21334>
- 588 8 Abraham, M. J. *et al.* GROMACS: High performance molecular simulations through
589 multi-level parallelism from laptops to supercomputers. *SoftwareX* **1-2**, 19-25 (2015).
590 <https://doi.org/10.1016/j.softx.2015.06.001>
- 591 9 Van Der Spoel, D. *et al.* GROMACS: fast, flexible, and free. *J Comput Chem* **26**, 1701-
592 1718 (2005). <https://doi.org/10.1002/jcc.20291>
- 593 10 Huang, J. *et al.* CHARMM36m: an improved force field for folded and intrinsically
594 disordered proteins. *Nat Methods* **14**, 71-73 (2017). <https://doi.org/10.1038/nmeth.4067>
- 595 11 Wang, J., Wang, W., Kollman, P. A. & Case, D. A. Automatic atom type and bond type
596 perception in molecular mechanical calculations. *J Mol Graph Model* **25**, 247-260
597 (2006). <https://doi.org/10.1016/j.jmgm.2005.12.005>
- 598 12 Salentin, S., Schreiber, S., Haupt, V. J., Adasme, M. F. & Schroeder, M. PLIP: fully
599 automated protein-ligand interaction profiler. *Nucleic Acids Res* **43**, W443-447 (2015).
600 <https://doi.org/10.1093/nar/gkv315>
- 601 13 Wenzel, M. *et al.* The Multifaceted Antibacterial Mechanisms of the Pioneering Peptide
602 Antibiotics Tyrocidine and Gramicidin S. *mBio* **9** (2018).
603 <https://doi.org/10.1128/mBio.00802-18>
- 604 14 Te Winkel, J. D., Gray, D. A., Seistrup, K. H., Hamoen, L. W. & Strahl, H. Analysis of
605 Antimicrobial-Triggered Membrane Depolarization Using Voltage Sensitive Dyes. *Front*
606 *Cell Dev Biol* **4**, 29 (2016). <https://doi.org/10.3389/fcell.2016.00029>
- 607 15 Schindelin, J. *et al.* Fiji: an open-source platform for biological-image analysis. *Nat*
608 *Methods* **9**, 676-682 (2012). <https://doi.org/10.1038/nmeth.2019>
- 609 16 Ducret, A., Quardokus, E. M. & Brun, Y. V. MicrobeJ, a tool for high throughput
610 bacterial cell detection and quantitative analysis. *Nat Microbiol* **1**, 16077 (2016).
611 <https://doi.org/10.1038/nmicrobiol.2016.77>
- 612 17 Schafer, A. B. *et al.* Dissecting antibiotic effects on the cell envelope using bacterial
613 cytological profiling: a phenotypic analysis starter kit. *Microbiol Spectr* **12**, e0327523
614 (2024). <https://doi.org/10.1128/spectrum.03275-23>
- 615 18 Anagnostopoulos, C. & Spizizen, J. Requirements for Transformation in *Bacillus*
616 *Subtilis*. *J Bacteriol* **81**, 741-746 (1961). <https://doi.org/10.1128/jb.81.5.741-746.1961>

- 617 19 Green, M. R. & Sambrook, J. Isolation of High-Molecular-Weight DNA Using Organic
618 Solvents. *Cold Spring Harb Protoc* **2017**, pdb prot093450 (2017).
619 <https://doi.org/10.1101/pdb.prot093450>
- 620 20 Singh, V. *et al.* Quantification of single-strand DNA lesions caused by the
621 topoisomerase II poison etoposide using single DNA molecule imaging. *Biochem*
622 *Biophys Res Commun* **594**, 57-62 (2022). <https://doi.org/10.1016/j.bbrc.2022.01.041>
- 623 21 Singh, V., Johansson, P., Lin, Y. L., Hammarsten, O. & Westerlund, F. Shining light on
624 single-strand lesions caused by the chemotherapy drug bleomycin. *DNA Repair (Amst)*
625 **105**, 103153 (2021). <https://doi.org/10.1016/j.dnarep.2021.103153>
- 626 22 Wei, Q. *et al.* Imaging and sizing of single DNA molecules on a mobile phone. *ACS*
627 *Nano* **8**, 12725-12733 (2014). <https://doi.org/10.1021/nn505821y>

628